XRD STUDIES ON SOLID STATE AMORPHISATION IN ELECTROLESS Ni/P AND Ni/B DEPOSITS

P. Sampath Kumar and P. Kesavan Nair,
Indian Institute of Technology, Madras
Madras- 600 036, India.

ABSTRACT

The decomposition of electroless Ni-P and Ni-B deposits on annealing at various temperatures is studied using x-ray diffraction techniques employing profile deconvolution and line profile analysis. It appears that solid state amorphisation takes place in the Ni-B deposits in a narrow temperature range just prior to the onset of crystallisation of amorphous phase. In the case of Ni-P deposits no evidence for solid state amorphisation could be obtained. Thermodynamic and kinetic considerations also support such a conclusion.

1.0 INTRODUCTION:

Considerable work has been done in recent years on metal-metal and metal-silicon diffusion couples. It has been shown that a metastable amorphous alloy phase may initially nucleate and grow by solid state amorphisation reactions(SSA) prior to the nucleation of crystalline intermetallics [1-4]. SSA was first observed in rhodium and amorphous silicon. Subsequently, the phenomenon has been observed in a number of metal-cation and metal-metal systems. SSA has been observed in many combinations, notably based on early/late transition metals. Major requirements or features of SSA have been summarized as follows:

1) Large heat of reaction between the two elements,
2) One of the elements is in general a fast diffuser in the other, establishing a diffusional asymmetry,
3) the thickness of the amorphous reaction layer which can form is limited,
4) formation of amorphous phase is favoured if a deep eutectic exists at the appropriate composition.

In most of the metal-metal or metal-cation systems, multilayered samples consisting of alternate layers of polycrystalline thin films of the two elements made by deposition or mechanical reduction have been used for studies. In such multilayer systems, study of interdiffusion is possible through a number of experimental techniques like Rutherford Back Scattering (RBS), thin films marker experiments, X-ray characterization etc. However, in the case of electroless or electrolytic deposits, these techniques are not suitable since the deposits lack lateral compositional homogeneity, unlike multilayered samples. Due to such difficulties of experimental detection, SSA in electroless deposits have not received adequate attention so far.

XRD techniques can profitably be employed in this case. Interaction between various phases can be followed through the relative intensities of diffraction profiles belonging to the respective phases, including amorphous phases. Modern profile deconvolution techniques can handle even heavily over lapping reflections which otherwise could be a serious limitation. In this study an attempt is made to study the SSA reactions in electroless nickel based deposits employing x-ray diffraction techniques.

2.0 EXPERIMENTAL:

2.1 Production of Deposits:

The deposition was carried out on mild steel substrates in the form of discs of 22.5 mm diameter and 7 mm thickness. The surface was polished to a metallographic finish using appropriate grades of emery paper and then electropolished using a solution of Perchloric acid (185 ml), Acetic anhydride (765 ml) and distilled water (45 ml). The thickness of the deposits were controlled primarily by adjusting the duration of deposition. The thickness achieved was about 30 microns.

2.11 Nickel Phosphorous Deposits:

For production of Ni-P deposits, nickel chloride was used as the source of nickel (30 g/l) and sodium hypophosphite as the reducing agent. The other ingredients used were sodium citrate (100 g/l) as the stabiliser and ammonium chloride (50 g/l) as the complexing agent. The amount of metalloid introduced into the deposit was controlled by varying the reducing agent in the plating solution from 10 g/l to 70 g/l. pH of the solution was adjusted with ammonia solution to a value 8 to 9. The temperature of deposition was 90 $\pm$ 1° C.

2.12 Nickel Boron Deposits:

In this case the plating solution had sodium borohydride as the reducing agent along with ethylenediamine (70 ml/l) as the complexing agent. The composition of the reducing agent was varied between 0.3 g/l and 0.7 g/l to control the boron content in the deposit. The pH of the solution was maintained above 13 using sodium hydroxide solution. Sodium citrate was the stabilising agent in this case also. The operating temperature was maintained at 90 $\pm$ 1° C.

2.2 Heat Treatment:

The deposits produced were annealed at 60, 100, 200, 300, 330, 360, 400, 500 and 600° C in the case of Ni-P. The Ni-B deposits on the other hand were annealed at 100, 150, 175, 200, 225, 250, 275, 300, 330, 400, 500 and 600° C. The annealing time was 2 hrs and no atmosphere was employed. The deposits were air cooled after annealing.

2.3 X-ray diffraction analysis:

2.31 Data Collection:

X-ray data were collected using a microprocessor controlled vertical goniometer. Filtered Co K radiation generated at 35 kV and 25 mA was employed. Both continuous scanning and step scanning were used. The continuous scans were performed at 1/2° (2θ) per minute. For step scans a step width of 0.03° (2θ) and a counting time of 5 sec/step was employed in all cases. To check whether the deposit thickness was sufficient to prevent the substrate effects vitiating the experimental data, the following criteria was employed: Since the most intense peaks of Ni and Fe (the (111) and (110) peaks respectively) have close angular positions for cobalt radiation, the disappearance of the second strong peak of the iron substrate (the (211) peak occurring at 99.7° (2θ)) was taken as the indication of negligible substrate effect.

2.32 Profile Analysis:

In the present investigations the x-ray diffraction profiles from electroless nickel deposits had contributions from both micro-crystalline nickel and amorphous phases. These profiles extensively overlapped with each other, in the as deposited conditions. Reflections corresponding to other crystalline phases like Ni_3P also begin to appear on annealing at higher temperatures. The ratios of the integrated intensities of amorphous and crystalline reflections could be used as an indicator of the relative proportions of the two phases. The (111) reflection from microcrystalline Ni along with the amorphous profile was used for this purpose. However it is essential that the reflections from the respective phases are separated with a reasonable level of accuracy and reproducibility. An iterative procedure described in detail else where [5], based on the computer program PRO-FIT [6] was employed.

The line profile analysis was carried out using the (111) and (222) reflections of nickel using well annealed powder as standard for instrumental corrections. Double line integral breadth analysis [7] and single line pseudo-Voigt analysis [8] were carried out using these reflections. Only in Ni-P deposits an identifiable (222) reflection from the samples in the as deposited condition could be obtained. Hence, double line integral breadth analysis was carried out only for Ni-P deposits in all temperatures of annealing. For Ni-B deposits until the appearance of (222) reflection, only single line analysis could be carried out.

3.0 RESULTS AND DISCUSSIONS:

A typical diffractogram obtained from the electroless Ni deposits is shown in Fig. 1. As can be seen the profiles from crystalline and amorphous peaks are overlapping extensively. Separated profiles from these phases are also shown. Variation of the ratio of integrated intensities of amorphous and crystalline reflections with annealing temperature for Ni-B deposits is shown in Fig.2a. The variation of the integral breadth of the Ni (111) reflection with annealing temperature is shown in Fig.2b. Corresponding results for Ni-P deposits are presented in Fig.3a and 3b. One can immediately see that the

response to annealing is not identical. In the case of Ni-B deposits, the ratio of integrated intensities of the amorphous and crystalline reflections show a significant and consistent increase just prior to the onset of equilibrium precipitates. In case of Ni-P deposits however the corresponding curve (Fig.3a.) shows only a more or less monotonic decrease. Similarly, while the integral breadth of Ni(111) reflection shows a slight decrease just prior to the onset of equilibrium precipitate, the corresponding curve for Ni-P deposits show only a continuous fall (Fig.3b)

To understand these differences, it might be worthwhile to go into the thermodynamic and kinetic aspects of SSA, as applied to these two systems. The basic thermodynamic requirement for the formation of an amorphous phase is that it leads to a decrease in the Gibbs' free energy (G). Even when this condition is satisfied, the amorphous phase so formed will only be metastable in the sense that equilibrium crystalline phases will have an even lower free energy leading to a further reduction in G on crystallization. However, such crystallization does not necessarily occur immediately due to kinetic constraints, which suppresses the crystalline phase formation. One such constraint could be the nucleation barrier. It has been suggested that in the case of crystallization, diffusion of both species are required (in a binary system). On the other hand, formation of amorphous phase requires the diffusion of just the faster moving species alone. Consequently, if there is a large difference in the mobilities or diffusivities of the two types of atoms, the energy required to move the slower moving atom may be regarded as the energy barrier, which prevents the crystalline phase formation.

In the present context, in both Ni-B and Ni-P systems, the slower moving atom happens to be nickel. It has been suggested that there is a clear correlation of smaller atomic radius with higher diffusivity in both metal-metal and metal-metalloid systems[9]. Consequently, due to the large difference in the atomic radius of P(0.11nm.) and B(0.046 nm) in relation to that of nickel(0.125 nm), the requirement of diffusional asymmetry is satisfied in the case of boron alone. In the case of phosphorous, the diffusion mechanism is likely to be nearer to the substitutional and in the case of boron interstitial.

To understand the relative stability of amorphous and crystalline phases, we first consider a possible variation of free energy(G) with composition for the amorphous phase and the solid solution of nickel and boron, shown in Fig.4a.

In this type of diagram, since part of the curve representing the amorphous phase (NiB_{am}) lies below the tangent line T_1T_2, the amorphous phase is stable and can coexist with the crystalline phase. Adopting the Gösele-Tu [10] criterion viz. maximizing

$$- d\Delta G/dt = - (d\Delta G/dx)(dx/dt) \qquad (1)$$

Where $d\Delta G/dx$ is driving force(per unit area of the product phase) and (dx/dt) is the rate of growth, one can note that in the case of NiB, the growth rate(dx/dt) is high due to the relatively faster rate of diffusion of boron and the absence of Ni_3B formation due to kinetic (nucleation) barriers. The result will be an increase in the amount of the amorphous phase, as the temperature rises, due to the higher mobility of boron. Diffusivity of nickel might still not be sufficient to start the formation of Ni_3B.

Once Ni_3B is formed, the free energy curve of the amorphous phase will be considerably at a higher level when compared to the relevant tangent line T_1T_3, shown in Fig.4b. The result will be a rapid decomposition of amorphous phase, once the crystalline phase (Ni_3B) has nucleated.

As per the Gösele-Tu criterion mentioned above, $(-d\Delta G/dx)$ is the driving force (per unit area) of interfacial reaction. If we assume that the driving force for formation of amorphous phase is not substantially different from that of crystalline phase, then the second factor, namely the rate of growth becomes the controlling factor for the stability of the amorphous phase. This implies that the amorphous phase becomes the favoured phase, if it has a higher growth rate; one obvious example is when the crystalline phase (in the present context Ni_3B) has not nucleated (ie. zero growth rate). However, the growth of amorphous phase is not impeded due to kinetic constraints such as nucleation barriers or low diffusivity.

The growth of the amorphous phase will require a continuous supply of boron from the existing nickel solid solution, resulting in a depletion of boron from the crystalline phase. This should in turn result in a decrease in the integral breadth of the Ni(111) reflection, concomitant with the increase in the I_{am}/I_{Ni} ratio. An examination of Figs. 2a and 2b shows that this indeed is the case..

In the case of Ni-P, the situation is different. In this case there is no increase in the I_{am}/I_{Ni} ratio on heating. On the other hand there is a more or less continuous decrease of the ratio, indicating the instability of the amorphous phase. A possible variation of free energy with composition in such a situation could be as shown in Fig.4c.

In this case the curve for the amorphous phase (Ni-P_{am}) is above the tangent line T_4T_5. The implication of this is that the equilibrium concentration range is now reversed (compare with Fig. 4a). Consequently the amorphous phase is inherently unstable. An increase in the mobility of the species (through an increase in temperature) will now result in a decrease in the amount of the amorphous phase. So long as the kinetic constraints prevent the formation of Ni_3P, the result will be a decrease in the I_{am}/I_{Ni} ratio. An examination of Fig.3a shows that this is broadly the case. However, a small increase in the I_{am}/I_{Ni} ratio at 100° C (Fig.3a), suggests that there is a narrow range with in which amorphous phase is still relatively stable. This could be because at this stage, the location of the free energy curve (Ni-P_{am}) might not be far above the tangent line or even just below the tangent line in this temperature range. The implication is that the reversal of the composition range takes place just above this temperature. Since the decomposition of the amorphous phase involves both the species, there need not be a relative increase in the phosphorous content of either the crystalline or amorphous phases. Consequently, the breadth of Ni(111) reflection will show only a decrease due to the lowering of lattice distortion caused by normal thermal effects. as shown in Fig.3b. In contrast, the decrease in the integral breadth of Ni(111) reflection in the case of Ni-B deposits (Fig.2b), occur at very narrow range of temperature. Introduction of the intermetallic (Ni_3P) will have a similar effect as in the case of Ni-B deposits. In this case also, once Ni_3P nucleates the decomposition of the amorphous phase will get accelerated and the completion of crystallisation will indeed be fast.

4.0 SUMMARY:

1) The decomposition behaviour of amorphous phase in electroless Ni-P and Ni-B systems are not identical.
2) In the case of Ni-P deposits, the amorphous phase content continuously decreases with temperature indicating no tendency for solid state amorphisation. In contrast Ni-B deposits have a small range of temperature just prior to the onset of recrystallisation of amorphous phase, wherein the amount of amorphous phase increases with temperature indicating a definite tendency for solid state amorphisation.
3) Thermodynamic and kinetic considerations behind the above conclusions are briefly examined.

References:

1. Schwarz.R and Johnson W.L: Phys. Rev. Lett., Vol.51, p415(1983)
2. Cahn. R.W. and Johnson W.L.: J. Mat. Res. Vol.1, p724(1986)
3. Herd.S, Tu.K.N and Ahn.K.Y.: Appl. Phys. Lett. Vol.42, p597(1983)
4. Holloway.K and Sinclair.R.: J. Appl. Phys. Vol.61, p1359 (1987)
5. Sampath Kumar.P. and Kesavan Nair. P.: NanoCrystaline Solids, vol4(2), p 183 (1994).
6. Hideo Toraya: `The Rietveld Method', Ed. Young. R.A, Publishers: International Union of Crystallography, Oxford University Press, p 254 (1993)
7. Rama Rao.P, Anantha Raman.T.R: Z.Metallkd., Vol. 62, p732 (1971)
8. Th. H. De Keijser, Mittemeijer. E.J and Rozendaal. H.C.F : J. Appl. Cryst. Vol.16, p309(1983)
9. Ricardo B. Schwarz : Proc. Int. Symposium on Advances in Phase Transitions, McMaster's University, Ontario, Canada, Oct. 22-23, 1987; Eds: Embury.J.D and Purdy. G.D, p.166 (1988)
10. Gösele. U and Tu. K.N: J. Appl. Phys. Lett., Vol.66(6), p2619 (1989)

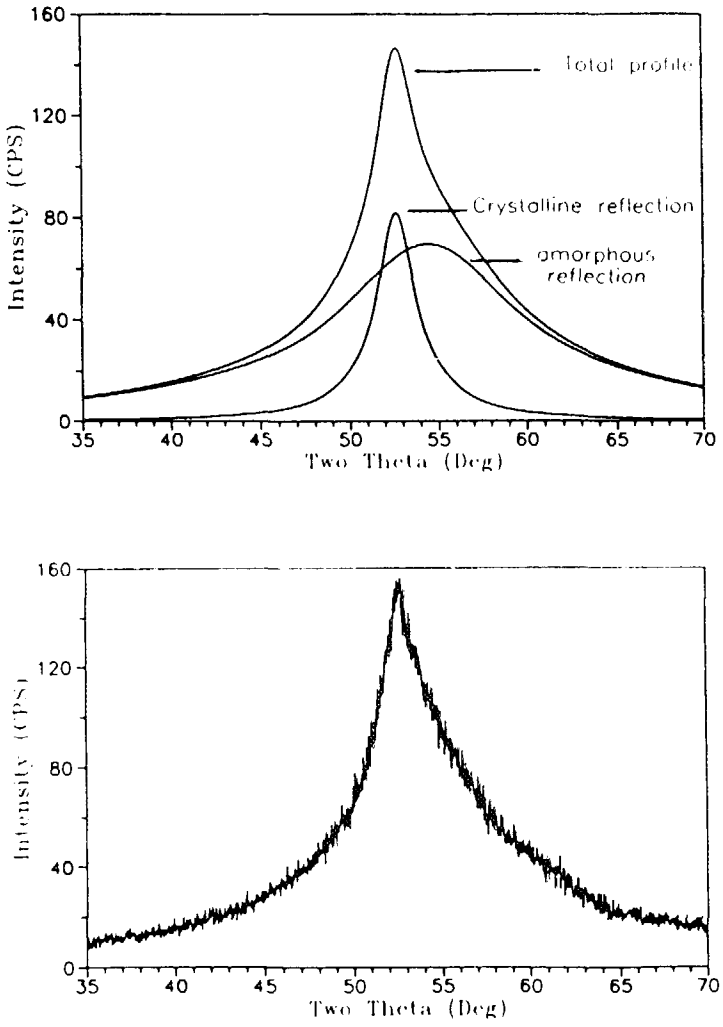

Fig. 1 Separation of amorphous and crystalline reflections. a) Experimental Profile. b) Separated profiles along with the total profile.

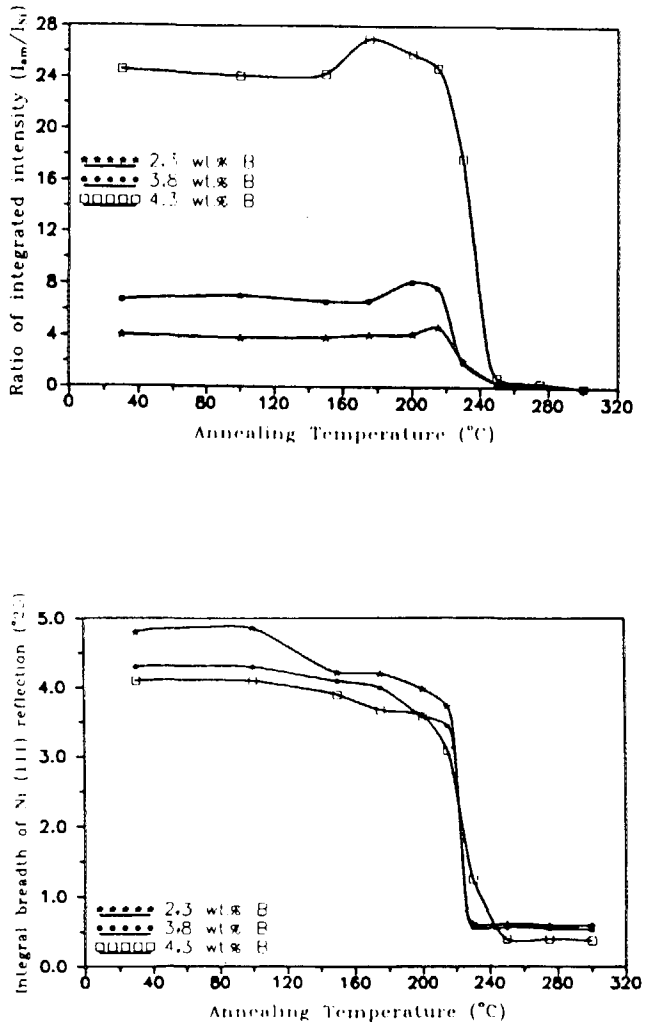

Fig. 2 Variation of a) ratio of integrated intensities of amorphous and crystalline reflections and b) integral breadth of (111) reflection, with annealing temperature in electroless Ni-B deposits.

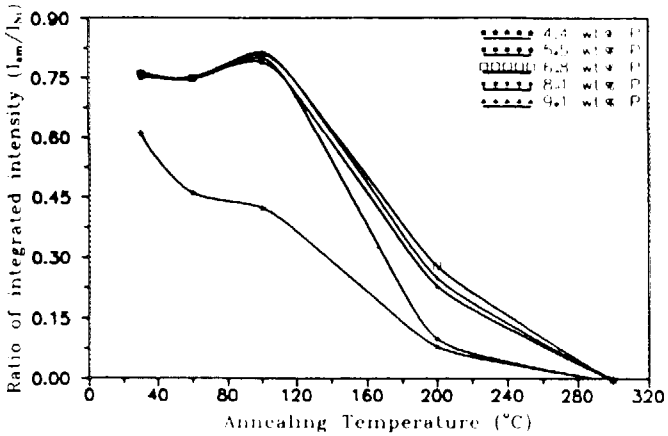

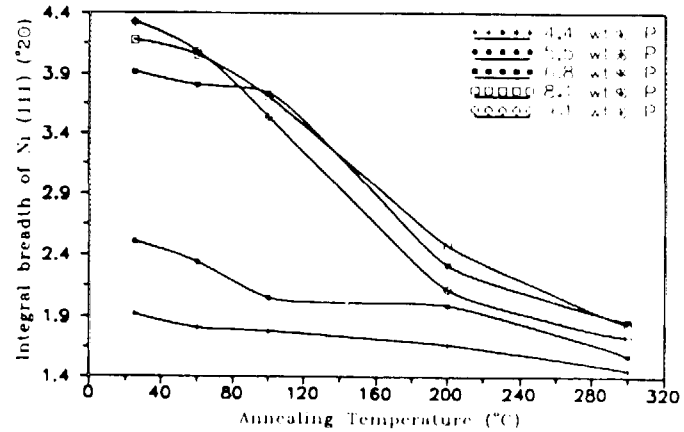

Fig. 3 Variation of a) ratio of integrated intensities of amorphous and crystalline reflections and b) integral breadth of (111) reflection, with annealing temperature in electroless Ni-P deposits.

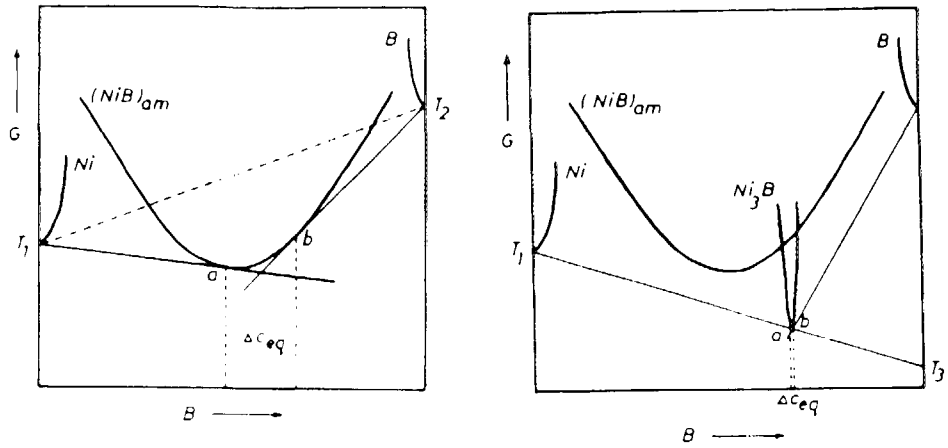

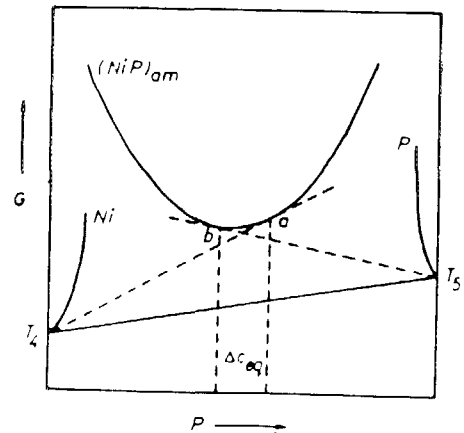

Fig. 4 Schematic variation of Gibbs' free energy with concentration for a) Ni-B system, prior to the onset of nucleation of Ni_3B and b) after the nucleation of Ni_3B. c) prior to the onset of nucleation of Ni_3P in Ni-P system.